

Scattering and delay time for 1D asymmetric potentials: The step-linear and the step-exponential case

Espalhamento e tempo de retardo para potenciais unidimensionais assimétricos:
Casos linear e exponencial por partes

L. Rizzi*^{1,2}, O.F. Piattella³, S.L. Cacciatori^{4,5}, V. Gorini⁶

¹Centre de Mathématiques Appliquées, Centre National de la Recherche Scientifique,
École Polytechnique, Paris, France

²Équipe Inventeurs du Monde Numérique GECO Saclay Île-de-France, Paris, France

³Departamento de Física, Universidade Federal do Espírito Santo, Vitória, ES, Brasil

⁴Dipartimento di Scienza e Alta Tecnologia, Università dell'Insubria, Como, Italy

⁵Istituto Nazionale di Fisica Nucleare, Sezione di Milano, Milano, Italy

⁶Dipartimento di Scienza e Alta Tecnologia, Università dell'Insubria, Como, Italy

Recebido em 12 de setembro de 2015. Aceito em 24 de outubro de 2015

We analyze the quantum-mechanical behavior of a system described by a one-dimensional asymmetric potential constituted by a step plus (i) a linear barrier or (ii) an exponential barrier. We solve the energy eigenvalue equation by means of the integral representation method, classifying the independent solutions as equivalence classes of homotopic paths in the complex plane. We discuss the structure of the bound states as function of the height U_0 of the step and we study the propagation of a sharp-peaked wave packet reflected by the barrier. For both the linear and the exponential barrier we provide an explicit formula for the delay time $\tau(E)$ as a function of the peak energy E . We display the resonant behavior of $\tau(E)$ at energies close to U_0 . By analyzing the asymptotic behavior for large energies of the eigenfunctions of the continuous spectrum we also show that, as expected, $\tau(E)$ approaches the classical value for $E \rightarrow \infty$, thus diverging for the step-linear case and vanishing for the step-exponential one.

Keywords: integral transforms, special functions, solutions of wave equations: bound states, scattering theory.

Analisamos o comportamento quântico de um sistema descrito por um potencial assimétrico unidimensional constituído por um degrau junto a (i) uma barreira linear ou (ii) uma barreira exponencial. Resolvemos a equação dos valores próprios da energia por meio do método da representação integral, classificando as soluções independentes como classes de equivalência de caminhos homotópicos no plano complexo. Discutimos a estrutura dos estados ligados como função da altura U_0 do degrau e estudamos a propagação de um pacote de onda pontiagudo refletido pela barreira. Para ambos os casos linear e exponencial fornecemos uma fórmula explícita para o retardo $\tau(E)$ como função da energia de pico E . Exibimos o comportamento ressonante de $\tau(E)$ para energias próximas de U_0 . Ao analisar o comportamento assintótico para grandes energias das funções próprias do espectro contínuo, mostramos também que, como esperado, $\tau(E)$ se aproxima do valor clássico para $E \rightarrow \infty$, divergindo assim para o caso linear e zerando para o caso exponencial.

Palavras-chave: transformações integrais, funções especiais, solução das equações de onda: estados ligados, teoria do espalhamento.

1. Introdução

In Ref. [1], we have analyzed the quantum-mechanical behavior of a system described by a one-

dimensional asymmetric potential formed by a step plus a harmonic barrier (the “step-harmonic” potential), by using the integral representation method [2]. We investigated the behavior of the discrete energy levels (as a function of the height of the step) and of the delay time τ of a wave packet coming from

*Endereço de correspondência:
luca.rizzi@cmap.polytechnique.fr.

infinity and bouncing back on the harmonic barrier, as a function of the packet’s peak energy and of the height U_0 of the step.

Among the convex or concave locally bounded symmetric and confining potentials the harmonic oscillator is a threshold, in that it gives rise to classical isochronous oscillations and evenly spaced quantum energy levels [3, 4].

In our quantum mechanical step variant of the problem we recover both these features in the limit in which $U_0 \rightarrow \infty$, and the potential reduces to the half-space harmonic oscillator. Then, it is conceivable that the harmonic one is the only confining barrier which displays a constant nonvanishing delay τ in the limit of high energies. For steeper barriers we expect τ to vanish at high energies, while for milder ones we expect the delay to become infinite in this limit, in accordance with the corresponding classical situations. Similarly, we expect that, as $U_0 \rightarrow \infty$, the spacing between two neighboring discrete levels tends to infinity in the former case and to zero in the latter.

Here we analyze the “step-linear” and the “step-exponential” potentials. Both these problems can be solved exactly using the integral representation method, which is interesting *per se*, as it can be applied to more general problems.

2. The step-linear potential

Let M, U_0 be positive parameters, and consider the “step-linear” potential

$$U(x) = \begin{cases} -Mx & x \leq 0, \\ U_0 & x > 0, \end{cases} \quad (1)$$

If E denotes the energy of the particle and m its mass, the time-independent Schrödinger equation is

$$-\frac{\hbar^2}{2m} \frac{d^2 u(x)}{dx^2} + U(x)u(x) = Eu(x). \quad (2)$$

This, for $x < 0$, can be rewritten as

$$\frac{d^2 u(x)}{dx^2} + \left(\frac{2mM}{\hbar^2} x + \frac{2mE}{\hbar^2} \right) u(x) = 0. \quad (3)$$

It is convenient to define

$$\alpha := \left(\frac{2mM}{\hbar^2} \right)^{1/3}, \quad \beta := \frac{\alpha E}{M}, \quad y := \alpha x, \quad (4)$$

which allows us to recast Eq. (3) as

$$\frac{d^2 u(y)}{dy^2} + (y + \beta) u(y) = 0, \quad (5)$$

which is the Airy equation (see Refs. [5, 6]). The general solution of Eq. (5) is

$$u(y) = CAi(-y - \beta) + DBi(-y - \beta), \quad (6)$$

where C and D are arbitrary integration constants, and the two linearly independent solutions Ai and Bi are expressed in section 5.1 in terms of the integral representation method.

Since $Bi(x) \rightarrow +\infty$ for $x \rightarrow +\infty$, in order for Eq. (6) to be an eigenfunction, we must set $D = 0$. Hence, we obtain

$$u(x) = CAi(-\alpha x - \beta). \quad (7)$$

For $x > 0$, the solution of Eq. (2) has the following form

$$u(x) = \begin{cases} Ae^{ikx} + Be^{-ikx} & E > U_0, \\ Fe^{-kx} & E < U_0, \end{cases} \quad (8)$$

where A, B and F are arbitrary integration constants and

$$\hbar k := \sqrt{2m|E - U_0|}. \quad (9)$$

2.1. The case $E < U_0$: Bound states and level spacing

If $E < U_0$ we obtain

$$u(x) = \begin{cases} CAi(-\alpha x - \beta) & x \leq 0, \\ Fe^{-kx} & x > 0. \end{cases} \quad (10)$$

The requirement of continuity of $u(x)$ and of its first derivative in $x = 0$ is expressed by

$$\begin{cases} CAi(-\beta) - F = 0, \\ C\alpha Ai'(-\beta) - Fk = 0. \end{cases} \quad (11)$$

System (11) has a non trivial solution iff

$$\frac{Ai'(-\beta)}{Ai(-\beta)} = \sqrt{\beta_0 - \beta}, \quad (12)$$

where $\beta_0 := \alpha U_0/M$. The energy levels are determined graphically by the intersections of the curves at the two sides of Eq. (12). An example is depicted in Fig. 1 for $\beta_0 = 6$.

In the limit $U_0 \rightarrow \infty$ the step of Eq. (1) becomes an infinite barrier. In this case, the energy levels correspond to the zeros β_n of $Ai(-\beta)$, the denominator of Eq. (12). As expected, these energy levels are the ones of the symmetric confining potential $U(x) = M|x|$ corresponding to the odd eigenfunctions of the latter (Appendix A).

To study the level separation for large energies, consider the asymptotics of $Ai(-\beta)$ for large values of β (see Ref. [7])

$$\text{Ai}(-\beta) = \frac{1}{\sqrt{\pi}\beta^{1/4}} \left[\sin\left(\zeta + \frac{\pi}{4}\right) \sum_{k=0}^{\infty} (-)^k c_{2k} \zeta^{-2k} - \cos\left(\zeta + \frac{\pi}{4}\right) \sum_{k=0}^{\infty} (-)^k c_{2k+1} \zeta^{-2k-1} \right], \quad (13)$$

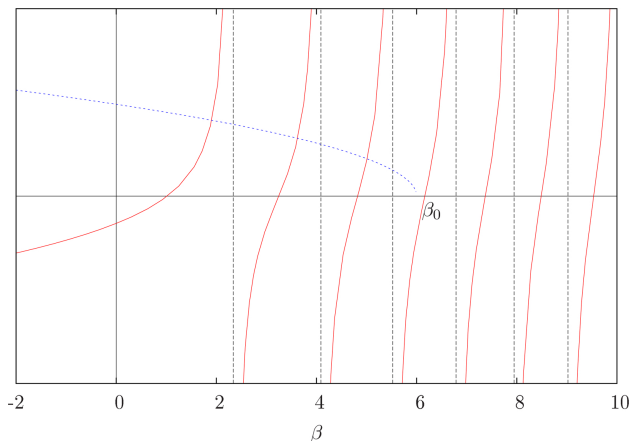


Figure 1: Graphical solutions of Eq. (12) for the energy levels. The red solid line represents the graph of the function $\text{Ai}'(-\beta)/\text{Ai}(-\beta)$ while the blue dash-dotted line represents the graph of $\sqrt{\beta_0 - \beta}$. In this plot, we have chosen $\beta_0 = 6$.

where $\zeta := 2\beta^{3/2}/3$ and the coefficients of the series expansions are given by

$$c_k = \frac{\Gamma\left(3k + \frac{1}{2}\right)}{54^k k! \Gamma\left(k + \frac{1}{2}\right)}. \quad (14)$$

The inversion of the asymptotic expansion (13) allows us to find, for large values of β , the following approximate solution of the equation $\text{Ai}(-\beta) = 0$ (see Ref. [7])

$$\begin{aligned} \beta_n &\sim t_n^{2/3} \left(1 + \frac{5}{48} \frac{1}{t_n^2} - \frac{5}{36} \frac{1}{t_n^4} + \dots \right), \\ t_n &= \frac{3}{8} \pi (4n - 1), \quad n \rightarrow \infty. \end{aligned} \quad (15)$$

Thus, at the leading order of Eq. (15) the approximate zeros have the form

$$\beta_n \simeq \left[\frac{3}{8} \pi (4n - 1) \right]^{2/3}. \quad (16)$$

This is an excellent approximation to the zeros of $\text{Ai}(-x)$ (see Table 1).

For $n \rightarrow \infty$ we get,

$$\beta_{n+1} - \beta_n \sim \left(\frac{8}{3n} \right)^{1/3} \pi^{2/3}, \quad n \rightarrow \infty. \quad (17)$$

The spacing behavior $n^{-1/3}$ is the threshold between concave and convex potentials.

Table 1: The first three zeros of the Airy function compared with the corresponding approximate zeros from Eq. (16).

n	β_n (exact)	β_n (approximate)	Relative Error
1	2.33811	2.32025	0.76×10^{-2}
2	4.08794	4.08181	0.15×10^{-2}
3	5.52055	5.51716	0.62×10^{-3}

2.2. The case $E > U_0$: Scattering and delay

In this case, the (improper) eigenfunctions have the form

$$u(x) = \begin{cases} C \text{Ai}(-\alpha x - \beta) & x \leq 0, \\ A e^{ikx} + B e^{-ikx} & x > 0. \end{cases} \quad (18)$$

The junction conditions in $x = 0$ are

$$\begin{cases} C \text{Ai}(-\beta) = A + B, \\ -C \alpha \text{Ai}'(-\beta) = ik(A - B). \end{cases} \quad (19)$$

Solving for the constants, the normalized (with respect to k) improper eigenfunctions are given by

$$u_k(x) = \frac{1}{\sqrt{2\pi}} \begin{cases} \Pi[\beta(k)] \text{Ai}[-\alpha x - \beta(k)] & x \leq 0, \\ e^{-ikx} + e^{ikx + i\delta(k)} & x > 0, \end{cases} \quad (20)$$

where

$$\begin{aligned} \Pi(\beta) &= 2 \left[\text{Ai}(-\beta) + \frac{\alpha}{ik} \text{Ai}'(-\beta) \right]^{-1}, \\ e^{i\delta(k)} &= \frac{ik \text{Ai}(-\beta) - \alpha \text{Ai}'(-\beta)}{ik \text{Ai}(-\beta) + \alpha \text{Ai}'(-\beta)}. \end{aligned} \quad (21)$$

As expected, the continuous part of the spectrum ($E > U_0$) is simple. Note that

$$\delta(k) = 2 \arctan \left[\frac{\alpha \text{Ai}'[-\beta(k)]}{k \text{Ai}[-\beta(k)]} \right]. \quad (22)$$

From Eq. (20) a generic wave packet

$$\psi(x, t) = \int_0^\infty dk c(k) u_k(x) e^{-\frac{i}{\hbar} E(k)t}. \quad (23)$$

has the form

$$\psi(x, t) = \frac{1}{\sqrt{2\pi}} \begin{cases} \int_0^\infty dk c(k) \Pi[\beta(k)] \text{Ai}[-\alpha x - \beta(k)] e^{-\frac{i}{\hbar} E(k)t} & x < 0, \\ \int_0^\infty dk c(k) [e^{ikx+i\delta(k)} + e^{-ikx}] e^{-\frac{i}{\hbar} E(k)t} = \psi_{\text{refl}} + \psi_{\text{in}} & x > 0. \end{cases} \quad (24)$$

Then, writing $c(k) = |c(k)|e^{i\gamma(k)}$, ψ_{in} and ψ_{refl} take the following form

$$\psi_{\text{in}}(x, t) = \frac{1}{\sqrt{2\pi}} \int_0^{+\infty} dk |c(k)| e^{-i[kx + \Omega(k)t - \gamma(k)]}, \quad (25)$$

$$\psi_{\text{refl}}(x, t) = \frac{1}{\sqrt{2\pi}} \int_0^{+\infty} dk |c(k)| e^{i[kx - \Omega(k)t + \delta(k) + \gamma(k)]}, \quad (26)$$

where

$$\Omega(k) := \frac{E(k)}{\hbar} = \frac{U_0}{\hbar} + \frac{\hbar k^2}{2m}. \quad (27)$$

If $c(k)$ is sufficiently regular and non-vanishing only in a small neighborhood of some \tilde{k} , then ψ_{in} and ψ_{refl} represent wave packets which move according to the following equations of motion [8, 9]

$$x_{\text{in}} = - \left. \frac{d\Omega}{dk} \right|_{k=\tilde{k}} t + \left. \frac{d\gamma}{dk} \right|_{k=\tilde{k}} = - \frac{\hbar \tilde{k}}{m} (t - t_0) = - \frac{\tilde{p}}{m} (t - t_0), \quad (28)$$

for the “incoming” wave packet, and

$$x_{\text{refl}} = \left. \frac{d\Omega}{dk} \right|_{k=\tilde{k}} t - \left. \frac{d\gamma}{dk} \right|_{k=\tilde{k}} - \left. \frac{d\delta}{dk} \right|_{k=\tilde{k}} = \frac{\tilde{p}}{m} \left[(t - t_0) - \frac{m}{\tilde{p}} \left. \frac{d\delta}{dk} \right|_{k=\tilde{k}} \right], \quad (29)$$

for the reflected “outgoing” one.

The solution thus built represents a particle of well defined momentum $\tilde{p} = \hbar \tilde{k}$ which approaches the origin from the right, interacts with the linear potential (at $t = t_0$), and is totally reflected. Note that the argument of the complex valued function $c(k)$ determines t_0 . The phase shift results in a delay τ in the rebound, caused by the interaction with the confining linear barrier. The delay is calculated with respect to the case of instantaneous reflection, which takes place in presence of an infinite barrier and for which $\delta(k) = \pi$. From Eqs. (4) and (9) it follows that

$$\tau(\tilde{\beta}) = \frac{\alpha \hbar}{M} \left. \frac{d\delta}{d\beta} \right|_{\beta=\tilde{\beta}}, \quad (30)$$

where $\tilde{\beta} := \beta(\tilde{k})$. We compute τ from Eq. (22). Using the Airy equation $\text{Ai}''(-\beta) = -\beta \text{Ai}(-\beta)$, we obtain

$$\tau(\beta) = \frac{\alpha \hbar}{M} \frac{2}{\sqrt{\beta - \beta_0} \frac{\text{Ai}(-\beta)}{\text{Ai}'(-\beta)} + \frac{1}{\sqrt{\beta - \beta_0}} \frac{\text{Ai}'(-\beta)}{\text{Ai}(-\beta)}} \left[-\frac{1}{2(\beta - \beta_0)} + \beta \frac{\text{Ai}(-\beta)}{\text{Ai}'(-\beta)} + \frac{\text{Ai}'(-\beta)}{\text{Ai}(-\beta)} \right], \quad (31)$$

where we have suppressed the tilde on the packet peak energy $\tilde{\beta}$.

We are interested in the behavior of the interaction time for large values of β , *i.e.* for incoming packets with high energy. To this end, we need the asymptotic expansion of $\text{Ai}'(-\beta)$ for $\beta \rightarrow +\infty$ (see Refs. [5, 7])

$$\text{Ai}'(-\beta) = -\frac{\beta^{1/4}}{\sqrt{\pi}} \left[\cos\left(\zeta + \frac{\pi}{4}\right) \sum_{k=0}^{\infty} (-)^k \frac{d_{2k}}{\zeta^{2k}} + \sin\left(\zeta + \frac{\pi}{4}\right) \sum_{k=0}^{\infty} (-)^k \frac{d_{2k+1}}{\zeta^{2k+1}} \right], \quad (32)$$

where $\zeta := 2\beta^{3/2}/3$ and the coefficients d_k are

$$d_k = -\frac{6k+1}{6k-1} c_k, \quad (33)$$

with c_k given in Eq. (14). Dividing the two asymptotic expansions of $\text{Ai}'(-\beta)$ and $\text{Ai}(-\beta)$ we obtain to leading order in β

$$\frac{1}{\sqrt{\beta - \beta_0}} \frac{\text{Ai}'(-\beta)}{\text{Ai}(-\beta)} \sim \tan\left(\frac{2}{3}\beta^{3/2} - \frac{\pi}{4}\right), \quad \beta \rightarrow \infty. \quad (34)$$

Thus, Eq. (31) becomes

$$\tau(\beta) \sim 2 \frac{\alpha \hbar}{M} \sqrt{\beta}, \quad \beta \rightarrow \infty. \quad (35)$$

Hence, reintroducing the physical variables, the high-energy behavior of the interaction time is

$$\tau(E) \sim \frac{2\sqrt{2mE}}{M}, \quad (36)$$

which is exactly the time a classical particle arriving from infinity with energy E would spend in the $x < 0$ region.

In Fig. 2 we plot $\tau(\beta)$ for a choice of different values of β_0 . Note the resonances located at the points $\beta \simeq \eta_n$ ($n = 1, 2, \dots$), zeros of $\text{Ai}'(-\beta)$, corresponding to the formation of metastable states at the respective energies $E_n \simeq M\eta_n/\alpha$. The values $M\eta_n/\alpha$ are the energies of the excited states of the confining potential $M|x|$ (see Appendix A), corresponding to even eigenfunctions. The resonances have lifetimes which decrease as the corresponding energies increase and move farther away from the threshold energy U_0 . Conversely, as U_0 increases, the lifetime of the resonance closest to the height of the step becomes progressively longer and then infinite when the resonance turns into the next bound state. This behavior is evident in Fig. 2, in which the first three plots correspond to values of β_0 for which there is only one bound state. In the successive three plots the resonance at $\beta \simeq \eta_1$ has disappeared, having turned into the second bound state.

Comparing Fig. 2 with Fig. 6 of Ref. [1] we note that, whereas in the step-harmonic case the graph of $\tau(\beta)$ oscillates with decreasing amplitude about the straight line $\tau = \pi/\omega$ (the half period of the oscillator), in the step-linear case the corresponding graph similarly oscillates about the parabolic line $\tau(E) = 2\sqrt{2mE}/M$, corresponding to the delay of the classical particle. Furthermore, whereas in the step-harmonic case the resonances are evenly spaced, in the step-linear case their spacing decreases with the energy, corresponding to the behavior as a function of the energy of the eigenvalues of the corresponding (symmetric) potentials $U(x) = m\omega^2 x^2/2$ and $U(x) = M|x|$.

3. The step-exponential potential

Let κ, σ and U_0 be positive parameters, and consider the “step-exponential” potential

$$U(x) = \begin{cases} \kappa \left(e^{-x/\sigma} - 1 \right) & x \leq 0, \\ U_0 & x > 0, \end{cases} \quad (37)$$

For $x < 0$, introduce the following dimensionless quantities

$$\alpha^2 := \frac{8m\kappa\sigma^2}{\hbar^2}, \quad \beta := \frac{8m(E + \kappa)\sigma^2}{\hbar^2}, \quad z := \alpha e^{-x/2\sigma}, \quad (38)$$

in terms of which the time-independent Schrödinger equation writes as

$$z^2 \frac{d^2 u(z)}{dz^2} + z \frac{du(z)}{dz} + (\beta - z^2) u(z) = 0. \quad (39)$$

Setting $\nu^2 := -\beta$, Eq. (39) can be cast in the form of a modified Bessel equation (see Ref. [5, 10])

$$z^2 \frac{d^2 u(z)}{dz^2} + z \frac{du(z)}{dz} - (\nu^2 + z^2) u(z) = 0, \quad (40)$$

whose general solution is

$$u(z) = CK_\nu(z) + DI_\nu(z), \quad (41)$$

where C and D are arbitrary integration constants and K_ν and I_ν are the modified Bessel functions of order $\nu = i\sqrt{\beta}$.

The function $I_\nu(z)$ diverges exponentially for $z \rightarrow +\infty$ [5]. For this reason, in order for $u(x)$ to be a proper (or improper) eigenfunction, we must set $D = 0$. Therefore Eq. (41) reduces to

$$u(x) = CK_{i\sqrt{\beta}} \left(\alpha e^{-x/2\sigma} \right). \quad (42)$$

Also the solutions of Eq. (40) can be studied with the integral representation method (see section 5.2).

3.1. The case $E < U_0$: Bound states

If $E < U_0$ we obtain

$$u(x) = \begin{cases} CK_{i\sqrt{\beta}} \left(\alpha e^{-x/2\sigma} \right) & x \leq 0, \\ Fe^{-kx} & x > 0. \end{cases} \quad (43)$$

The junction conditions in $x = 0$ give

$$\alpha K'_{i\sqrt{\beta}}(\alpha) = 2\sigma k K_{i\sqrt{\beta}}(\alpha), \quad (44)$$

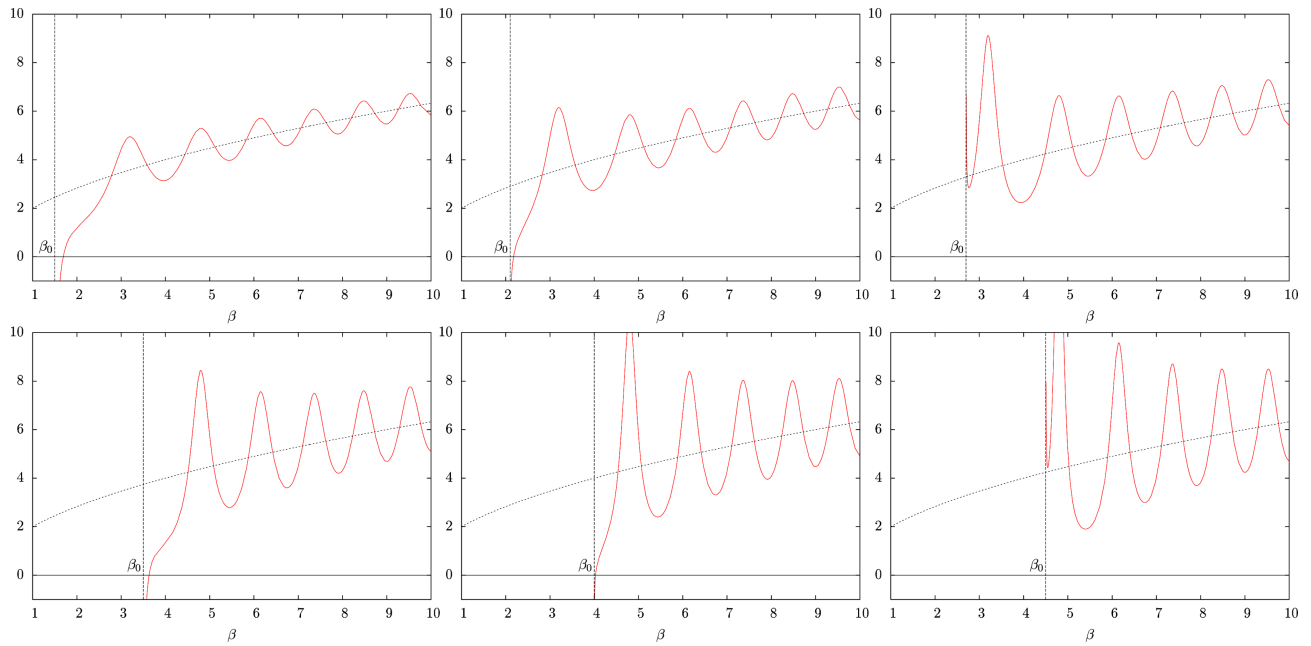


Figure 2: Plots of the delay τ (in units of $\hbar\alpha/M$) versus the energy β of the incoming wave packet (red solid lines) for $\beta_0 = 1.5, 2.1, 2.7, 3.5, 4.0, 4.5$. The parabolic blue dotted lines represent the classical delay, given in Eq. (36).

which, setting $\beta_0 := 8m(U_0 + \kappa)\sigma^2/\hbar^2$ can be recast in the form

$$\frac{K'_{i\sqrt{\beta}}(\alpha)}{K_{i\sqrt{\beta}}(\alpha)} = \frac{\sqrt{\beta_0 - \beta}}{\alpha}. \tag{45}$$

Graphical solutions of Eq. (45) are shown in Fig. 3.

Analogously to what happens in the step-linear case (12), in the limit of an infinite barrier ($U_0 \rightarrow$

∞) the energy levels are specified by the zeros of $K_{i\sqrt{\beta}}(\alpha)$, the denominator of Eq. (44), as a function of β and they are the ones of the symmetric confining potential $U(x) = \kappa(e^{|x|/\sigma} - 1)$, corresponding to the odd eigenfunctions of the latter (Appendix B).

To study how the energy levels behave for large energies, we employ the following formula for the asymptotic behavior of the function $K_{i\sqrt{\beta}}(\alpha)$ for large β (see Ref. [5])

$$K_{i\sqrt{\beta}}(\alpha) \sim \sqrt{\frac{2\pi}{\sqrt{\beta}}} e^{-\pi\sqrt{\beta}/2} \sin \left[\frac{\alpha^2}{4\sqrt{\beta}} - \sqrt{\beta} + \sqrt{\beta} \log \left(\frac{2\sqrt{\beta}}{\alpha} \right) + \frac{\pi}{4} \right] \left[1 + O \left(\frac{1}{\sqrt{\beta}} \right) \right], \tag{46}$$

for $\beta \rightarrow \infty$. Note that expansion (46) can be proved starting from Eq. (76). Therefore, the zeros of $K_{i\sqrt{\beta}}(\alpha)$, as a function of β , are asymptotically the solutions of the following equation

$$-\sqrt{\beta_n} + \sqrt{\beta_n} \log \left(\frac{2\sqrt{\beta_n}}{\alpha} \right) = n\pi. \tag{47}$$

Solving for β_n we obtain

$$\beta_n \sim \frac{\alpha^2 e^2}{4} \exp \left[2W \left(\frac{2n\pi}{\alpha e} \right) \right], \tag{48}$$

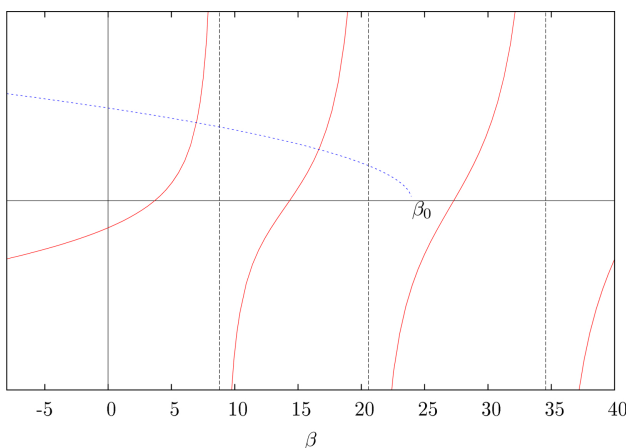


Figure 3: Graphical solutions of (45). The red solid line is the graph of $K'_{i\sqrt{\beta}}(\alpha)/K_{i\sqrt{\beta}}(\alpha)$, whereas the blue dash-dotted line represents $\sqrt{\beta_0 - \beta}/\alpha$ for the choice $\beta_0 = 24$ and $\alpha = 1$.

where $W(x)$ is the Lambert function [5]. Since $W(x) \sim \log x - \log \log x$ for $x \rightarrow \infty$ we have for large n that

$$\beta_n \sim \frac{n^2 \pi^2}{\left(\log \frac{2n\pi}{\alpha e}\right)^2}. \tag{49}$$

We see from Eq. (49) that the potential $U(x) = \kappa \left(e^{|x|/\sigma} - 1\right)$ behaves for large x as an infinite square well whose width, up to inessential factors, grows as $\log n$, an intuitive fact. Moreover,

$$\beta_{n+1} - \beta_n \sim \frac{2n\pi^2}{\left(\log \frac{2n\pi}{\alpha e}\right)^2}, \tag{50}$$

for $n \rightarrow \infty$, proving thus that the level spacing diverges.

3.2. The case $E > U_0$: Scattering and delay

The unbound eigenstates have the form

$$u(x) = \begin{cases} CK_{i\sqrt{\beta}}(\alpha e^{-x/2\sigma}) & x \leq 0, \\ Ae^{ikx} + Be^{-ikx} & x > 0. \end{cases} \tag{51}$$

Then, following the same argument adopted for the step-linear case, we obtain the following formula for the delay τ of the rebound of an incoming wavepacket with peak energy β

$$\tau(\beta) = \frac{8m\sigma^2}{\hbar} \frac{d\delta}{d\beta} = \frac{8m\sigma^2}{\hbar} \frac{2}{\frac{\sqrt{\beta-\beta_0}}{\alpha} \frac{K_{i\sqrt{\beta}}(\alpha)}{K'_{i\sqrt{\beta}}(\alpha)} + \frac{\alpha}{\sqrt{\beta-\beta_0}} \frac{K'_{i\sqrt{\beta}}(\alpha)}{K_{i\sqrt{\beta}}(\alpha)}} \left[-\frac{1}{2(\beta-\beta_0)} + \frac{d}{d\beta} \log \frac{K'_{i\sqrt{\beta}}(\alpha)}{K_{i\sqrt{\beta}}(\alpha)} \right]. \tag{56}$$

Using Eq. (46), we obtain for large values of β

$$\frac{K'_{i\sqrt{\beta}}(\alpha)}{K_{i\sqrt{\beta}}(\alpha)} \sim -\frac{\sqrt{\beta}}{\alpha} \cot \left(-\sqrt{\beta} + \sqrt{\beta} \log \frac{2\sqrt{\beta}}{\alpha} + \frac{\pi}{4} \right), \tag{57}$$

from which

$$\frac{d}{d\beta} \log \frac{K'_{i\sqrt{\beta}}(\alpha)}{K_{i\sqrt{\beta}}(\alpha)} \sim \frac{1}{2\beta} - \frac{1}{\sin \left[2 \left(-\sqrt{\beta} + \sqrt{\beta} \log \frac{2\sqrt{\beta}}{\alpha} + \frac{\pi}{4} \right) \right]} \frac{1}{\sqrt{\beta}} \log \frac{2\sqrt{\beta}}{\alpha}. \tag{58}$$

A comment is here in order. In general, taking the derivative of an asymptotic expansion with respect to the variable or a parameter may lead to wrong results. However, in our case this procedure can be justified using the integral representation

and the junction conditions are

$$\begin{cases} CK_{i\sqrt{\beta}}(\alpha) = A + B, \\ C\alpha K'_{i\sqrt{\beta}}(\alpha) = i2\sigma k(B - A). \end{cases} \tag{52}$$

Therefore, the normalized (with respect to k) improper eigenfunctions are given by

$$u_k(x) = \frac{1}{\sqrt{2\pi}} \begin{cases} \Pi[\beta(k)] K_{i\sqrt{\beta(k)}}(\alpha e^{-x/2\sigma}) & x \leq 0, \\ e^{ikx+i\delta(k)} + e^{-ikx} & x > 0, \end{cases} \tag{53}$$

where $\hbar k = \sqrt{2m(E - U_0)}$ and

$$\begin{aligned} \Pi(\beta) &= 2 \left[K_{i\sqrt{\beta}}(\alpha) + \frac{\alpha}{2ik\sigma} K'_{i\sqrt{\beta}}(\alpha) \right]^{-1}, \tag{54} \\ e^{i\delta(k)} &= \frac{2ik\sigma K_{i\sqrt{\beta}}(\alpha) - \alpha K'_{i\sqrt{\beta}}(\alpha)}{2ik\sigma K_{i\sqrt{\beta}}(\alpha) + \alpha K'_{i\sqrt{\beta}}(\alpha)}. \end{aligned}$$

Hence,

$$\delta(k) = 2 \arctan \left[\frac{\alpha}{2\sigma k} \frac{K'_{i\sqrt{\beta(k)}}(\alpha)}{K_{i\sqrt{\beta(k)}}(\alpha)} \right]. \tag{55}$$

of Eq. (77) (we leave this as an exercise for the interested reader).

Thus, plugging Eq. (58) into Eq. (56) we obtain the asymptotic behavior of the delay time for large

β 's, namely

$$\tau(\beta) \sim \frac{8m\sigma^2}{\hbar} \frac{1}{\sqrt{\beta}} \log\left(\frac{2\sqrt{\beta}}{\alpha}\right), \quad (59)$$

or, in terms of the energy of the particle

$$\tau(E) \sim \frac{2\sigma \log(2E/\kappa)}{\sqrt{2E/m}}. \quad (60)$$

As expected, Eq. (60) coincides with the large energy value of the half period of the classical particle subjected to the confining potential $U(x) = \kappa(e^{|x|/\sigma} - 1)$.

4. Conclusions

Regarding the structure of the discrete energy spectrum as a function of the height U_0 of the barrier, in the two potentials treated in this paper, the same considerations apply as those of the concluding section of Ref. [1]. The only difference is that the energy levels $\hbar\omega(n + 1/2)$, $n \in \mathbb{N}$, of the harmonic oscillator have to be replaced here by the corresponding levels E_n of the confining linear and exponential potentials, respectively (see Appendices A and B). In the case of the step-linear potential, the level spacing Eq. (17) goes to zero as the energy increases, while in the case of the step-exponential one (50) it approaches infinity. As regards the continuous spectrum, we provide in both cases exact expressions for the delay of a wavepacket reflected from the barrier, as a function of the peak packet energy (see Eqs. (31) and (56)). As expected, in both cases these delays exhibit a series of resonances for energies not much larger than U_0 , while for large energies, they approach the classical values. The step-harmonic potential is a threshold separating the potential barriers for which the delay time goes to infinity at large energies from those for which it vanishes.

An entirely similar discussion can be applied to the step variant

$$U(x) = \begin{cases} V(x) & x \leq 0, \\ U_0 & x > 0, \end{cases} \quad (61)$$

of any symmetric potential $V(x)$ ($V(x) = V(-x)$) such that $\lim_{x \rightarrow \pm\infty} V(x) = +\infty$. Indeed the energy eigenvalue equation for $V(x)$ has two linearly independent solutions $u_L(x)$ and $v_L(x)$ the first of which approaches zero very rapidly as $x \rightarrow -\infty$

whereas the second one diverges steadily without oscillating, and two linearly independent solutions $u_R(x)$ and $v_R(x)$ having a corresponding behavior for $x \rightarrow +\infty$ (see Refs. [8, 11]). Since $u_L(x) = a(E)u_R(x) + b(E)v_R(x)$, the energy eigenvalues are the roots E_n of the equation $b(E) = 0$. Since the potential is symmetric, these roots correspond to even and odd eigenfunctions alternatively, the ground state being even. However, in the general case the eigenvectors cannot be found explicitly. Therefore, for example, no explicit formula is available in general for the delay time of the reflected packet in the corresponding step variant potential (61).

5. Airy and modified Bessel functions through the integral representations

In this section we solve the energy eigenvalue equations by means of the integral representation method, classifying the independent solutions as equivalence classes of homotopic paths in the complex plane. For the step-linear case we obtain Airy function, while for the step-exponential case we get modified Bessel functions. This technique is interesting *per se*, as it can be applied to more general cases, provided one is able to guess the correct integral kernel. The Airy case is somehow classical, while the Bessel case is more interesting. We present them both for completeness.

5.1. The step-linear case: Airy functions

We look for a solution of Eq. (5) of the form

$$E(y) = \int_{\gamma} dt f(t) e^{ty}, \quad (62)$$

where γ is a path in the complex plane and f is an holomorphic function. Plugging Eq. (62) into Eq. (5) we find

$$\int_{\gamma} dt \left[(t^2 + \beta) f(t) e^{ty} + \frac{de^{ty}}{dy} f(t) \right] = 0. \quad (63)$$

Integrating by parts, we obtain:

$$\left[e^{ty} f(t) \right]_{\partial\gamma} + \int_{\gamma} dt \left[(t^2 + \beta) f(t) - f(t)' \right] e^{ty} = 0. \quad (64)$$

Therefore, $E(y)$ is a solution of Eq. (5) if

$$\left[e^{ty} f(t) \right]_{\partial\gamma} = 0 \quad \text{and} \quad f(t) = \exp\left(\frac{t^3}{3} + \beta t\right). \quad (65)$$

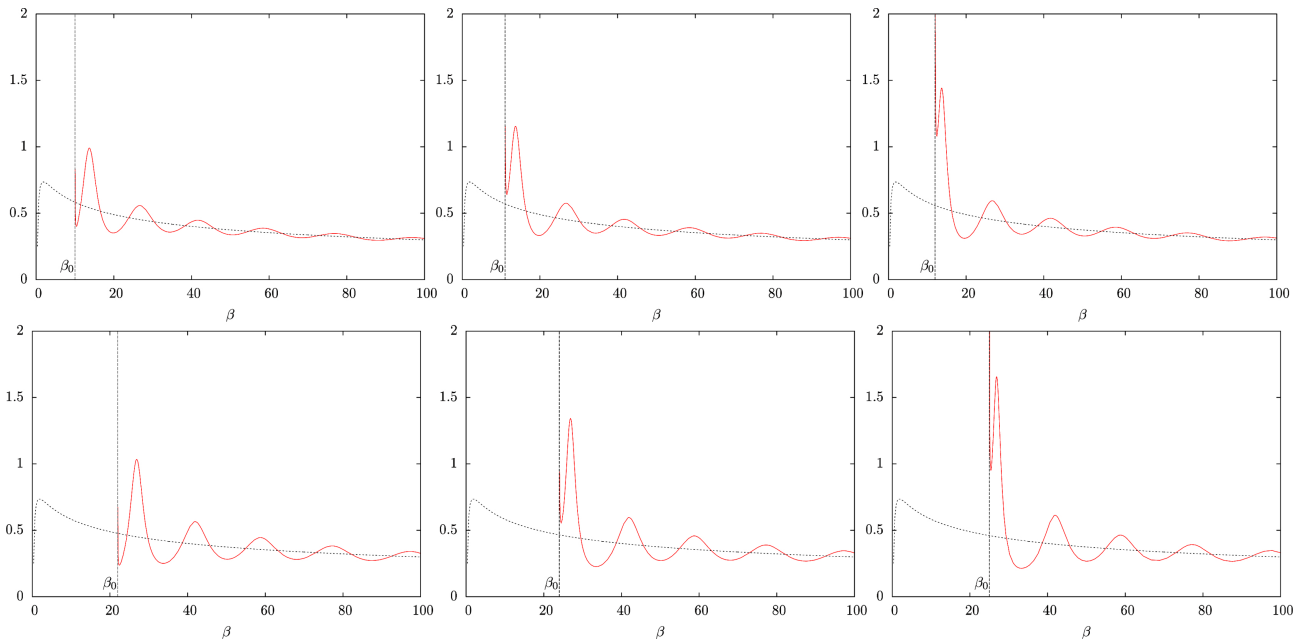


Figure 4: Plots of the delay τ (in units of $8m\sigma^2/\hbar$) versus the energy β of the incoming wave packet (solid red lines) for six values of the step height: $\beta_0 = 10, 11, 12$ (upper panels) $\beta_0 = 22, 24, 25$ (lower panels). The blue dotted lines represent the classical delay.

Hence, a class of solutions of the Airy equation is of the form

$$E_\beta(y) = \int_\gamma dt \exp \left[\frac{t^3}{3} + (\beta + y)t \right], \quad (66)$$

where γ is a suitable path for which the contour term vanishes.

The integrand of Eq. (66) entire. Thus, by Cauchy theorem, every closed path represents the trivial solution $E(y) = 0$.

Consider an unbounded path. In order for $[e^{ty}f(t)]_{\partial\gamma}$ to vanish, we require the leading term in the exponent of $f(t)$ (i.e. t^3) to have a negative real part. Therefore, the acceptable unbounded paths are those whose phase ϕ is confined to the regions $\frac{\pi}{6} < \phi + \frac{2}{3}n\pi < \frac{\pi}{2}$ ($n = 0, 1, 2$). These possible paths are showed in Fig. 5, where the allowed sectors $\frac{\pi}{6} < \phi + \frac{2}{3}n\pi < \frac{\pi}{2}$ ($n = 0, 1, 2$) are shaded.

Paths with both endpoints in the same sector (e.g. Γ_4 in Fig. 5) can be closed at infinity using Jordan’s Lemma; therefore, they correspond to the trivial solution. The only non-trivial paths are those which link different sectors. There are only 3 non-equivalent classes of such paths which we dub Γ_1 , Γ_2 and Γ_3 respectively (see Fig. 5).

Taking into account Cauchy theorem, these paths satisfy the relation $\Gamma_1 + \Gamma_2 = \Gamma_3$ in the sense that the corresponding solutions are not independent. The

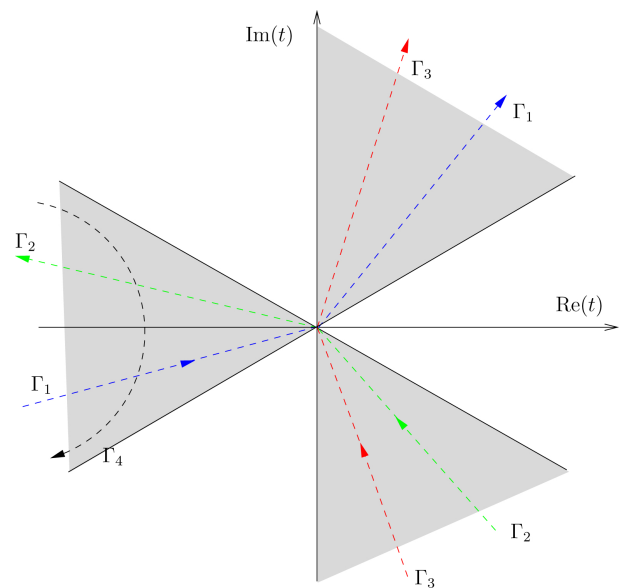


Figure 5: Possible paths of integration, each one corresponding to a solution of (5).

conventional Airy functions $\text{Ai}(z)$ and $\text{Bi}(z)$ are the independent solutions of $w''(z) - zw'(z) = 0$ such that (see Ref. [5])

$$\text{Ai}(0) = \frac{3^{-2/3}}{\Gamma(2/3)}, \quad \text{Ai}'(0) = -\frac{3^{-1/3}}{\Gamma(1/3)}, \quad (67)$$

and

$$\text{Bi}(0) = \sqrt{3} \frac{3^{-2/3}}{\Gamma(2/3)}, \quad \text{Bi}'(0) = \sqrt{3} \frac{3^{-1/3}}{\Gamma(1/3)}.$$

Denoting by $E_\beta^{(i)}(y)$ the solutions in Eq. (66) corresponding to the paths Γ_i ($i = 1, 2$), it is not difficult to show that

$$\begin{aligned} \text{Ai}(-y - \beta) &= \frac{1}{2\pi i} [E_\beta^{(1)}(y) + E_\beta^{(2)}(y)], \\ \text{Bi}(-y - \beta) &= \frac{1}{2\pi} [E_\beta^{(1)}(y) - E_\beta^{(2)}(y)]. \end{aligned} \quad (68)$$

We leave the details to the interested reader (*hint*: Check the above expressions and their first derivatives in Eq. (66) for $y = \beta = 0$. In this case the integrals $E_0^{(j)}(0)$ correspond to Euler Gamma functions).

5.2. The step-exponential case: Modified Bessel functions

Consider the modified Bessel equation

$$z^2 u''(z) + zu'(z) - (\nu^2 + z^2)u(z) = 0, \quad (69)$$

with $z > 0$. A convenient kernel for the integral representation is the following:

$$K(z, t) = z^\nu e^{-z \cosh t}. \quad (70)$$

We look for solutions of the form

$$u(z) = \int_\gamma dt f(t) K(z, t). \quad (71)$$

Plugging Eq. (71) into Eq. (69), we get

$$\begin{aligned} z^{\nu+1} \int_\gamma dt \left[f(t) \frac{d}{dt} (\sinh(t) e^{-z \cosh t}) + \right. \\ \left. 2\nu f(t) \cosh(t) e^{-z \cosh t} \right] = 0. \end{aligned} \quad (72)$$

Integrating by parts, Eq. (72) gives

$$\begin{aligned} & \left[z^{\nu+1} e^{-z \cosh t} f(t) \sinh(t) \right]_{\partial\gamma} - \\ & z^{\nu+1} \int_\gamma dt [f'(t) \sinh(t) - 2\nu f(t) \cosh(t)] e^{-z \cosh t} \\ & = 0. \end{aligned} \quad (73)$$

Then, the integral on the right hand side of Eq. (71) is a solution of Eq. (69) if

$$\begin{aligned} f'(t) \sinh(t) - 2\nu f(t) \cosh(t) &= 0, \quad \text{and} \\ z^{\nu+1} \left[e^{-z \cosh t} f(t) \sinh(t) \right]_{\partial\gamma} &= 0. \end{aligned} \quad (74)$$

Up to a normalization, the solution is $f(t) = \sinh(t)^{2\nu}$. If ν is integer then $f(t)$ is either entire ($\nu \geq 0$) or meromorphic ($\nu < 0$), otherwise it has infinite branch points located at $t_n = in\pi$ ($n = 0, \pm 1, \dots$), see Fig. 6. In the latter instance, the usual procedure is to define a domain in which the function is holomorphic by cutting the t -plane and thus forbidding loops around the branch points. In Fig. 6 a convenient choice for the cuts is also shown.

Recalling that $\text{Re}(z) > 0$, the contour condition $z^{\nu+1} \left[e^{-z \cosh(t)} f(t) \sinh(t) \right]_{\partial\gamma} = 0$ is

$$e^{-z \cosh t} \sinh(t)^{2\nu+1} |_{\partial\gamma} = 0. \quad (75)$$

There are 4 different classes of paths for which Eq. (75) is satisfied and

$$u(z) = \int_\gamma \sinh(t)^{2\nu} e^{-z \cosh t} z^\nu dt, \quad (76)$$

is well defined. The ‘‘paths zoology’’ is more complicated and rich than in the linear and in the harmonic case [1].

1. **Closed paths.** For any closed path, the contour condition is trivially satisfied and any integral along a path enclosing a region where the integrand function is holomorphic (i.e. the path does not cross the cuts) vanishes. An example is shown by the thin dashed black line in Fig. 6.
2. **Infinite paths.** For paths whose endpoints are both at infinity, the function $\sinh(t)^{2\nu+1}$

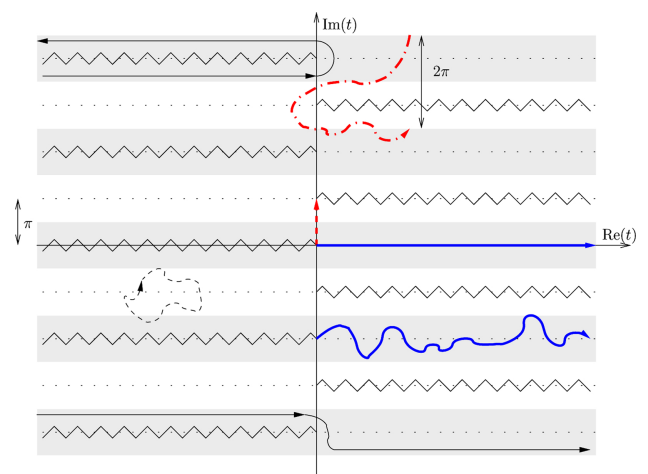


Figure 6: Cut of the complex t -plane. The dashed red and the solid blue thick paths represent the only classes of paths which provide independent solutions to the modified Bessel equation.

diverges or oscillates. On the other hand, the exponential $e^{-z \cosh t}$ vanishes for $\text{Re}(\cosh t) \rightarrow +\infty$ (recall that $z > 0$). Since $\text{Re}[\cosh(x+iy)] = \cos(y) \cosh(x)$ then γ must stretch at infinity in one of the sectors defined by $-\pi/2 + 2n\pi < \text{Im}(t) < \pi/2 + 2n\pi$ ($n = 0, \pm 1, \dots$), which are represented by the shaded regions in Fig. 6. Incidentally, in these bands, when there are no cuts, one can “close” the paths at infinity, by virtue of Jordan’s Lemma. Examples of this class of paths are the black solid thin lines of Fig. 6.

3. **Semi-infinite paths.** By “semi-infinite” paths we mean paths starting from a point, say t_0 , and ending at infinity. These paths must go to infinity in the shaded bands $-\pi/2 + 2n\pi < \text{Im}(t) < \pi/2 + 2n\pi$. For the starting point t_0 , the contour condition demands that $\sinh(t_0)^{2\nu+1} = 0$. This means that these paths must start from one of the points $t_n = in\pi$, which are the zeroes of the hyperbolic sine function. It is easy to prove that the integral of Eq. (76) performed along any two such paths lying in the same band gives the same result (indeed, recall that $\sinh t$ is periodic). Two examples of this class of paths are the blue solid thick lines in Fig. 6.
4. **Finite paths.** These are the paths starting and ending in two points say t_i and t_f , with $|t_i|, |t_f| < \infty$. The contour condition can be satisfied in two different ways: either the values of the contour part are equal at the endpoints, or the contour part vanishes at the endpoints. The former case accounts for paths which do not cross any cut and start from any point t_i , ending at $t_f = t_i + 2ni\pi$ ($n = 0, \pm 1, \dots$). Examples of this class of paths are represented by the red dash-dotted thick line in Fig. 6. The latter case is realized by paths connecting the branch points and is represented by the red dashed thick line in Fig. 6.

Taking into account the periodicity of the integrand function (the period is $2\pi i$ in the domain where it is holomorphic), and the Cauchy theorem, it is easy to show that the integrals along the two kinds of finite paths are proportional to the integral along the “fundamental” path $[0, i\pi]$. Moreover, the integrals along any one of the infinite paths are linear combinations of the ones performed along the finite and semi-infinite paths.

In conclusion, two linear independent solutions of Eq. (69) are

$$K_\nu(z) = \frac{\pi^{1/2}(z/2)^\nu}{\Gamma(\nu + 1/2)} \int_0^\infty dx e^{-z \cosh x} \sinh(x)^{2\nu}, \tag{77}$$

and

$$I_\nu(z) = \frac{(z/2)^\nu}{\pi^{1/2}\Gamma(\nu + 1/2)} \int_0^\pi dx e^{-z \cos x} \sin(x)^{2\nu}, \tag{78}$$

where K_ν and I_ν correspond, respectively, to the integrals performed along the solid blue and the dashed red thick lines in Fig. 6 (a semi-infinite path and a finite one). It can be shown that both solutions (derived here for $z > 0$) can be analytically continued throughout the whole z -plane cut along the negative real axis (see Ref. [2]).

6. Appendix

A. The confining symmetric linear potential

Consider the confining symmetric potential $U(x) = M|x|$. The eigenfunctions can be written as

$$\begin{cases} u(x) = C_1 \text{Ai}(-\alpha x - \beta) & x < 0, \\ u(x) = C_2 \text{Ai}(\alpha x - \beta) & x > 0, \end{cases} \tag{79}$$

where C_1 and C_2 are constants fixed by the junction conditions in $x = 0$. If $\text{Ai}(-\beta) \neq 0$, then the continuity of $u(x)$ in $x = 0$ implies $C_1 = C_2$. Moreover, the continuity of the derivative implies $\text{Ai}'(-\beta) = 0$. This condition determines the *even* eigenfunctions and their eigenvalues. If $\text{Ai}(-\beta) = 0$, then the continuity of the derivative implies $C_1 = -C_2$. This condition determines the *odd* eigenfunctions and their eigenvalues.

B. The confining symmetric exponential potential

Consider the confining symmetric potential $U(x) = \kappa(e^{|x|/\sigma} - 1)$. The eigenfunctions can be written as

$$\begin{cases} u(x) = C_1 K_{i\sqrt{\beta}}(\alpha e^{-x/2\sigma}) & x < 0, \\ u(x) = C_2 K_{i\sqrt{\beta}}(\alpha e^{x/2\sigma}) & x > 0, \end{cases} \tag{80}$$

where C_1 and C_2 are constants fixed by the junction conditions in $x = 0$. If $K_{i\sqrt{\beta}}(\alpha) \neq 0$, then the continuity of $u(x)$ in $x = 0$ implies $C_1 = C_2$. Moreover,

the continuity of the derivative implies $K'_{i\sqrt{\beta}}(\alpha) = 0$. This condition determines the *even* eigenfunctions and their eigenvalues. If $K_{i\sqrt{\beta}}(\alpha) = 0$, then the continuity of the derivative implies $C_1 = -C_2$. This condition determines the *odd* eigenfunctions and their eigenvalues.

References

- [1] L. Rizzi, O.F. Piattella, S.L. Cacciatori and V. Gorini, *Am. J. Phys.* **78**, 842 (2010).
- [2] H. Hochstadt, *The Functions of Mathematical Physics* (Dover Publications, New York, 1976), p. 100-105.
- [3] J.F. Cariñena, A.M. Perelomov and M.F. Rañada, *J. Phys. Conf. Ser.* **87**, 012007 (2007).
- [4] M. Asorey, J.F. Cariñena, G. Marmo and A. Perelomov, *Annals Phys.* **322**, 1444 (2007).
- [5] M. Abramowitz and I.A. Stegun, *Handbook of Mathematical Functions* (Dover Publications, New York, 1972), 10th. ed.
- [6] O. Vallée and M. Soares, *Airy Functions and Applications to Physics* (Imperial College Press, London, 2004).
- [7] B.R. Fabijonas and F.W.J. Olver, *SIAM Review* **41**, 762 (1999).
- [8] P. Caldirola, R. Cirelli and G.M. Prosperi, *Introduction to Theoretical Physics* (UTET, Milano, 1982) 1st. ed. (in Italian).
- [9] D.J. Griffiths, *Introduction to Quantum Mechanics* (Benjamin Cummings, San Francisco, 2004), 2nd. ed.
- [10] G.N. Watson, *A Treatise on the Theory of Bessel Functions* (Cambridge University Press, Cambridge, 1966), 2nd. ed.
- [11] F.G. Tricomi, *Differential Equations* (Einaudi, Torino, 1953), 2d ed. (in Italian).